Localized waves of the coupled cubic–quintic nonlinear Schrödinger equations in nonlinear optics*

Tao Xu(徐涛)[1,3], Yong Chen(陈勇)[1,2,3,†], and Ji Lin(林机)[2]

[1] Shanghai Key Laboratory of Trustworthy Computing, East China Normal University, Shanghai 200062, China
[2] Department of Physics, Zhejiang Normal University, Jinhua 321004, China
[3] MOE International Joint Laboratory of Trustworthy Software, East China Normal University, Shanghai 200062, China

(Received 5 July 2017; revised manuscript received 12 August 2017; published online 20 October 2017)

We investigate some novel localized waves on the plane wave background in the coupled cubic–quintic nonlinear Schrödinger (CCQNLS) equations through the generalized Darboux transformation (DT). A special vector solution of the Lax pair of the CCQNLS system is elaborately constructed, based on the vector solution, various types of higher-order localized wave solutions of the CCQNLS system are constructed via the generalized DT. These abundant and novel localized waves constructed in the CCQNLS system include higher-order rogue waves, higher-order rogues interacting with multi-soliton or multi-breather separately. The first- and second-order semi-rational localized waves including several free parameters are mainly discussed: (i) the semi-rational solutions degenerate to the first- and second-order vector rogue wave solutions; (ii) hybrid solutions between a first-order rogue wave and a dark or bright soliton, a second-order rogue wave and two dark or bright solitons; (iii) hybrid solutions between a first-order rogue wave and a breather, a second-order rogue wave and two breathers. Some interesting and appealing dynamic properties of these types of localized waves are demonstrated, for example, these nonlinear waves merge with each other markedly by increasing the absolute value of α. These results further uncover some striking dynamic structures in the CCQNLS system.

Keywords: generalized Darboux transformation, localized waves, soliton, rogue wave, breather, coupled cubic–quintic nonlinear Schrödinger equations

PACS: 02.30.IK, 03.75.Nt, 31.15.–p **DOI:** 10.1088/1674-1056/26/12/120201

1. Introduction

In recent years, nonlinear localized waves, including solitons,[1–3] rogue waves,[4–7] and breathers,[8–10] have been one of the intense studies in the field of nonlinear science. Many attentions have been focused on the common solitons including bright and dark solitons. Owing to the instability of small amplitude perturbations, the breathers may develop and even grow in size to disastrous proportions. In much current literature, there are mainly two kinds of breathers such as Ma breathers (time-periodic breather solutions)[11] and Akhmediev breathers (space-periodic breather solutions).[4,12] While the rogue waves are modeled as transient wave packets localized in both time and space, they reveal a unique phenomenon that seems to appear from nowhere and disappear without a trace.[13] Up to now, the authentic interpretations of the generation mechanism of the rogue waves are modulation instability and rational function solution.[14] The rogue wave phenomenon appears in a class of fields, among them nonlinear optics,[15,16] capillary flow,[17] superfluidity,[18] Bose–Einstein condensates,[19] plasma physics,[20] and even finance.[21]

Recent studies have been extended to localized wave solutions including rogue waves and some other nonlinear wave in various nonlinear systems.[22–24] In Ref. [25], the hybrid solutions consisted of rogue waves and cnoidal periodic waves in the focusing NLS equation were constructed by the Darboux transformation (DT) scheme. Using the Hirota bilinear method, the authors obtained the rogue wave triggered by the interaction between lump soliton and a pair of resonance kink stripe solitons.[26,27] As one special type of interactional solutions, the semi-rational solution exhibits a range of abundant and appealing dynamics in nonlinear models,[28] such as dark–bright–rogue wave pair,[29,30] rogue wave interacting with solitons and breathers.[31–33] In many cases, it shows that these semi-rational solutions appear as a mixture of polynomials with exponential functions. In Ref. [34], a new dark–antidark soliton pair solutions and some special semi-rational solutions of the coupled Sasa–Satsuma equations were discussed by DT. Utilizing the Hirota bilinear method, the authors constructed a new kind of semi-rational solution that the rogue waves interact with solitons and breathers at the same time in the Boussinesq equation.[35] These results further uncover some striking dynamic structures in nonlinear models.

It is necessary to generate shorter (femtosecond, even attosecond) pulses with high frequency in fibre to meet the demand for high bit rates in optical communication. In the field of ultra-short pulses, where the width of optical pulse is in

*Project supported by the Global Change Research Program of China (Grant No. 2015CB953904), the National Natural Science Foundation of China (Grant Nos. 11675054 and 11435005), the Shanghai Collaborative Innovation Center of Trustworthy Software for Internet of Things (Grant No. ZF1213), and the Natural Science Foundation of Hebei Province, China (Grant No. A2014210140).

†Corresponding author. E-mail: ychen@sei.ecnu.edu.cn

© 2017 Chinese Physical Society and IOP Publishing Ltd

the order of femtosecond (10^{-15} s) and the spectrum of these ultrashort pulses is approximately of the order 10^{15} s^{-1}, the standard NLS equation is less accurate. This boosts greatly the study of higher order nonlinear effects in optics, which are modeled by various higher order NLS systems. In this paper, our aim is to investigate the localized waves of the following coupled cubic–quintic nonlinear Schrödinger (CCQNLS) equations[36–39]

$$\begin{aligned}
&\mathrm{i}q_{1t}+q_{1xx}+2(|q_1|^2+|q_2|^2)q_1+(\rho_1|q_1|^2+\rho_2|q_2|^2)^2q_1-2\mathrm{i}[(\rho_1|q_1|^2+\rho_2|q_2|^2)q_1]_x+2\mathrm{i}(\rho_1q_1^*q_{1x}+\rho_2q_2^*q_{2x})q_1=0,\\
&\mathrm{i}q_{2t}+q_{2xx}+2(|q_1|^2+|q_2|^2)q_2+(\rho_1|q_1|^2+\rho_2|q_2|^2)^2q_2-2\mathrm{i}[(\rho_1|q_1|^2+\rho_2|q_2|^2)q_2]_x+2\mathrm{i}(\rho_1q_1^*q_{1x}+\rho_2q_2^*q_{2x})q_2=0,
\end{aligned}\tag{1}$$

which describe the effects of quintic nonlinearity on the ultrashort optical pulse propagation in non-Kerr media. For convenience, the independent variables z and t of the CCQNLS equations in Refs. [36]–[39] are replaced by variables t and x in the CCQNLS system (1), respectively. The two components q_1 and q_2 are the complex smooth envelop functions and they denote that two electromagnetic fields propagate along the coordinate z (or t) in the two cores of an optical waveguide, and t (or x)is the local time. Besides, each non-numeric subscripted variable stands for partial differentiation and the asterisk denotes complex conjugation. The parameters ρ_1 and ρ_2 are all real constants. When $q_1=u$, $q_2=0$, and $\rho_1=2\beta$, the CCQNLS system (1) can turn into the integrable Kundu–Eckhaus equation.[40] There have been many reports on the Kundu–Eckhaus equation,[41] such as its Hamiltonian structure,[42] solitons solutions,[43] and rogue wave solutions.[44,45] Recently, the multi-soliton solutions and the bound states of the solitons of the CCQNLS system (1) were discussed in Refs. [36] and [37]. In Ref. [38], the authors constructed the generalized DT of the CCQNLS system and obtained its rogue wave solutions. Besides, the DT of the multi-component CCQNLS system were obtained and its rogue waves were also constructed.[39]

Here, we are interested in the hybrid solutions between rogue waves and some other nonlinear wave solutions in the CCQNLS system (1), for example, multi-dark, multi-bright soliton, and multi-breather. To the best of our knowledge, there are no reports on this kind of interactional solution of the CCQNLS system up to the present. Baronio *et al.*[46] obtained some semi-rational solutions in the coupled NLS, which include a first-order rogue wave, a first-order rogue wave interacting with a bright soliton, a dark soliton, and a breather, respectively. However, the higher-order interactional solutions cannot be generated by Baronio's method. Based on the generalized DT[14,47] and the special vector solution of the Lax pair of the three-component coupled NLS system, we obtained its higher-order interactional solutions successfully.[31] Starting from an appropriate periodic seed solution, a special vector solution of the Lax pair of the system (1) is elaborately constructed. Based on this kind of special vector solution, some abundant higher-order localized waves of the CCQNLS equations are generated by the generalized DT. In particular, the first- and second-order semi-rational localized wave solutions are discussed in detail. These semi-rational localized wave solutions are discussed in three cases: the first one is the first- and second-order vector rogue wave solutions; the second one is the hybrid solutions between a first-order rogue wave and a dark or bright soliton, a second-order rogue wave and two dark or bright solitons; the last one is the interactional solutions between a first-order rogue wave and a breather, a second-order rogue wave and two breathers. These interesting and appealing solutions will further reveal some striking dynamic structures in the CCQNLS system.

Our paper is organized as follows. In Section 2, we construct the generalized DT to Eq. (1), then the first- to fourth-step generalized Darboux transformations are obtained by using the direct iterative rule. In Section 3, some nonlinear localized wave solutions of Eq. (1) are obtained. In particular, the first- and second-order localized waves are discussed in detail and some figures of these kinds of localized wave solutions are also exhibited. In Section 4, we give some conclusions.

2. Generalized Darboux transformation

In this section, we construct the generalized DT[14,47] to the CCQNLS system (1). The Lax pair of the system (1) can be expressed as[38,39]

$$\boldsymbol{\Psi}_x=\boldsymbol{U}\boldsymbol{\Psi},\quad \boldsymbol{\Psi}_t=\boldsymbol{V}\boldsymbol{\Psi},\tag{2}$$

where $\boldsymbol{\Psi}=(\psi(x,t),\phi(x,t),\chi(x,t))^{\mathrm{T}}$ with T denoting the transpose of the vector, while $\boldsymbol{U}$ and $\boldsymbol{V}$ are all the 3×3 matrices and they can be given as

$$\boldsymbol{U}=\begin{bmatrix}
-\mathrm{i}\lambda+\frac{1}{2}\mathrm{i}(\rho_1|q_1|^2+\rho_2|q_2|^2) & q_1 & q_2\\
-q_1^* & \mathrm{i}\lambda-\frac{1}{2}\mathrm{i}(\rho_1|q_1|^2+\rho_2|q_2|^2) & 0\\
-q_2^* & 0 & \mathrm{i}\lambda-\frac{1}{2}\mathrm{i}(\rho_1|q_1|^2+\rho_2|q_2|^2)
\end{bmatrix},$$

$$\boldsymbol{V}=\begin{bmatrix}\omega+\mathrm{i}(|q_1|^2+|q_2|^2) & s_1 & s_2\\ \mathrm{i}q_{1x}^*-2\lambda q_1^*-q_1^*(\rho_1|q_1|^2+\rho_2|q_2|^2) & -\omega-\mathrm{i}|q_1|^2 & -\mathrm{i}q_2q_1^*\\ \mathrm{i}q_{2x}^*-2\lambda q_2^*-q_2^*(\rho_1|q_1|^2+\rho_2|q_2|^2) & -\mathrm{i}q_1q_2^* & -\omega-\mathrm{i}|q_2|^2\end{bmatrix},$$

where

$$\begin{aligned}\omega&=-2\mathrm{i}\lambda^2+\mathrm{i}(\rho_1|q_1|^2+\rho_2|q_2|^2)^2\\&\quad+\frac{1}{2}\rho_1(q_1q_{1x}^*-q_{1x}q_1^*)+\frac{1}{2}\rho_2(q_2q_{2x}^*-q_{2x}q_2^*),\\ s_1&=2\lambda q_1+(\rho_1|q_1|^2+\rho_2|q_2|^2)q_1+\mathrm{i}q_{1x},\\ s_2&=2\lambda q_2+(\rho_1|q_1|^2+\rho_2|q_2|^2)q_2+\mathrm{i}q_{2x},\end{aligned}$$

and λ is the spectral parameter. Besides, the CCQNLS system (1) can be derived from the compatibility condition $\boldsymbol{U}_t-\boldsymbol{V}_x+[\boldsymbol{U},\boldsymbol{V}]=0$ through symbolic computation, where the brackets represent the matrix commutator.

Let $\boldsymbol{\Psi}_1=(\psi_1,\phi_1,\chi_1)^{\mathrm{T}}$ be a special solution of the Lax pair (2) with $q_1=q_1[0]$, $q_2=q_2[0]$, and $\lambda=\lambda_1$, then based on the DT constructed in Refs. [36]– [38], we give the first-step elementary DT of the CCQNLS equations (1)

$$\boldsymbol{\Psi}[1]=\boldsymbol{\Gamma}\boldsymbol{T}\boldsymbol{\Psi},$$

$$\boldsymbol{T}=\lambda\boldsymbol{I}-\boldsymbol{H}\boldsymbol{\Lambda}\boldsymbol{H}^{-1}=(\lambda-\lambda_1^*)\boldsymbol{I}+(\lambda_1^*-\lambda_1)\frac{\boldsymbol{\Psi}_1\boldsymbol{\Psi}_1^{\dagger}}{\boldsymbol{\Psi}_1^{\dagger}\boldsymbol{\Psi}_1},\quad(3)$$

$$q_1[1]=\mathrm{e}^{2\eta}(q_1[0]+\frac{2\mathrm{i}(\lambda_1^*-\lambda_1)\psi_1\phi_1^*}{\boldsymbol{\Omega}}),\quad(4)$$

$$q_2[1]=\mathrm{e}^{2\eta}(q_2[0]+\frac{2\mathrm{i}(\lambda_1^*-\lambda_1)\psi_1\chi_1^*}{\boldsymbol{\Omega}}),\quad(5)$$

where

$$\boldsymbol{I}=\begin{pmatrix}1&&\\&1&\\&&1\end{pmatrix},\ \boldsymbol{\Gamma}=\begin{pmatrix}\mathrm{e}^{\eta}&&\\&\mathrm{e}^{-\eta}&\\&&\mathrm{e}^{-\eta}\end{pmatrix},$$

$$\Lambda=\begin{pmatrix}\lambda_1&&\\&\lambda_1^*&\\&&\lambda_1^*\end{pmatrix},\ \boldsymbol{H}=\begin{pmatrix}\psi_1&\phi_1^*&\chi_1^*\\\phi_1&-\psi_1^*&0\\\chi_1&0&-\psi_1^*\end{pmatrix},$$

$$\boldsymbol{\Omega}=|\psi_1|^2+|\phi_1|^2+|\chi_1|^2,\quad\eta=\int(\lambda_1-\lambda_1^*)\,\boldsymbol{\Omega}^{-2}\boldsymbol{\Delta}\,\mathrm{d}x,$$

$$\begin{aligned}\boldsymbol{\Delta}&=\rho_1[\,(q_1[0]\phi_1\psi_1^*+q_1[0]^*\phi_1^*\psi_1)\,\boldsymbol{\Omega}\\&\quad+2\mathrm{i}(\lambda_1^*-\lambda_1)|\psi_1|^2|\phi_1|^2]+\rho_2[\,(q_2[0]\chi_1\psi_1^*\\&\quad+q_2[0]^*\chi_1^*\psi_1)\boldsymbol{\Omega}+2\mathrm{i}(\lambda_1^*-\lambda_1)|\psi_1|^2|\chi_1|^2],\end{aligned}$$

the symbol † denotes the transpose and complex conjugation of the vector.

According to the above elementary DT expressions (3)–(5), we construct the generalized DT to the CCQNLS equations(1). Let $\boldsymbol{\Psi}_1=(\psi_1,\phi_1,\chi_1)^{\mathrm{T}}=\boldsymbol{\Psi}_1(\lambda_1+\delta)$ be a special vector solution of the Lax pair (2) with $q_1=q_1[0]$, $q_2=q_2[0]$, $\lambda=\lambda_1+\delta$, and δ is a small parameter. Next, $\boldsymbol{\Psi}_1$ can be expanded as the Taylor series at $\delta=0$

$$\boldsymbol{\Psi}_1=\boldsymbol{\Psi}_1^{[0]}+\boldsymbol{\Psi}_1^{[1]}\delta+\boldsymbol{\Psi}_1^{[2]}\delta^2+\cdots+\boldsymbol{\Psi}_1^{[N]}\delta^N+\cdots,\quad(6)$$

where

$$\boldsymbol{\Psi}_1^{[l]}=(\psi_1^{[l]},\phi_1^{[l]},\chi_1^{[l]})^{\mathrm{T}},\ \boldsymbol{\Psi}_1^{[l]}=\frac{1}{l!}\frac{\partial^l\boldsymbol{\Psi}_1}{\partial\delta^l}|_{\delta=0},\ (l=0,1,2,3,\ldots).$$

By means of the formulas (3)–(6), the first-step generalized DT of Eq. (1) can be directly constructed. In the following content of this section, we use these notations $\boldsymbol{D}[j]=\boldsymbol{\Gamma}_1^{[j]}\boldsymbol{T}[j]$, $\boldsymbol{D}_1[j]=\boldsymbol{\Gamma}_1^{[j]}\boldsymbol{T}_1[j]$, and $\boldsymbol{T}_1[j]=\boldsymbol{T}[j]|_{\lambda=\lambda_1}=\lambda_1\boldsymbol{I}-\boldsymbol{H}[j-1]\boldsymbol{\Lambda}_1\boldsymbol{H}[j-1]^{-1}$, $(j=1,2,3,\ldots,N)$.

(i) The first-step generalized DT

$$\boldsymbol{\Psi}[1]=\boldsymbol{D}[1]\boldsymbol{\Psi}=\boldsymbol{\Gamma}_1^{[1]}\boldsymbol{T}[1]\boldsymbol{\Psi},\quad(7)$$

$$\begin{aligned}\boldsymbol{T}[1]&=\lambda\boldsymbol{I}-\boldsymbol{H}[0]\boldsymbol{\Lambda}_1\boldsymbol{H}[0]^{-1}\\&=(\lambda-\lambda_1^*)\boldsymbol{I}+(\lambda_1^*-\lambda_1)\frac{\boldsymbol{\Psi}_1[0]\boldsymbol{\Psi}_1[0]^{\dagger}}{\boldsymbol{\Psi}_1[0]^{\dagger}\boldsymbol{\Psi}_1[0]},\end{aligned}\quad(8)$$

$$q_1[1]=\mathrm{e}^{2\eta_1^{[1]}}\Big(q_1[0]+\frac{2\mathrm{i}(\lambda_1^*-\lambda_1)\psi_1[0]\phi_1[0]^*}{\boldsymbol{\Omega}_1}\Big),\quad(9)$$

$$q_2[1]=\mathrm{e}^{2\eta_1^{[1]}}\Big(q_2[0]+\frac{2\mathrm{i}(\lambda_1^*-\lambda_1)\psi_1[0]\chi_1[0]^*}{\boldsymbol{\Omega}_1}\Big),\quad(10)$$

where $\boldsymbol{\Psi}_1[0]=\boldsymbol{\Psi}_1^{[0]}=(\psi_1[0],\phi_1[0],\chi_1[0])^{\mathrm{T}}$,

$$\boldsymbol{\Gamma}_1^{[1]}=\begin{pmatrix}\mathrm{e}^{\eta_1^{[1]}}&&\\&\mathrm{e}^{-\eta_1^{[1]}}&\\&&\mathrm{e}^{-\eta_1^{[1]}}\end{pmatrix},\ \boldsymbol{\Lambda}_1=\begin{pmatrix}\lambda_1&&\\&\lambda_1^*&\\&&\lambda_1^*\end{pmatrix},$$

$$\boldsymbol{H}[0]=\begin{pmatrix}\psi_1[0]&\phi_1[0]^*&\chi_1[0]^*\\\phi_1[0]&-\psi_1[0]^*&0\\\chi_1[0]&0&-\psi_1[0]^*\end{pmatrix},$$

$$\boldsymbol{\Omega}_1=|\psi_1[0]|^2+|\phi_1[0]|^2+|\chi_1[0]|^2,$$

$$\eta_1^{[1]}=\int(\lambda_1-\lambda_1^*)\,\boldsymbol{\Omega}_1^{-2}\boldsymbol{\Delta}_1\,\mathrm{d}x,$$

$$\begin{aligned}\boldsymbol{\Delta}_1&=\rho_1[\,(q_1[0]\phi_1[0]\psi_1[0]^*+q_1[0]^*\phi_1[0]^*\psi_1[0])\,\boldsymbol{\Omega}_1\\&\quad+2\mathrm{i}(\lambda_1^*-\lambda_1)|\psi_1[0]|^2|\phi_1[0]|^2]+\rho_2[\,(q_2[0]\chi_1[0]\psi_1[0]^*\\&\quad+q_2[0]^*\chi_1[0]^*\psi_1[0])\,\boldsymbol{\Omega}_1+2\mathrm{i}(\lambda_1^*-\lambda_1)|\psi_1[0]|^2|\chi_1[0]|^2].\end{aligned}$$

(ii) The second-step generalized DT

It is shown that $\boldsymbol{T}[1]\boldsymbol{\Psi}_1$ is a vector solution of the Lax pair (2) with $q_1=q_1[1]$, $q_2=q_2[1]$, and $\lambda=\lambda_1+\delta$. Considering the following limit

$$\begin{aligned}\lim_{\delta\to0}\frac{\boldsymbol{D}[1]|_{\lambda=\lambda_1+\delta}\Psi_1}{\delta}&=\lim_{\delta\to0}\frac{\boldsymbol{\Gamma}_1^{[1]}(\delta+\boldsymbol{T}_1[1])\boldsymbol{\Psi}_1}{\delta}\\&=\boldsymbol{\Gamma}_1^{[1]}(\boldsymbol{\Psi}_1^{[0]}+\boldsymbol{T}_1[1]\boldsymbol{\Psi}_1^{[1]})\equiv\boldsymbol{\Psi}_1[1],\end{aligned}\quad(11)$$

a nontrivial solution of the Lax pair (2) with $q_1=q_1[1]$, $q_2=q_2[1]$, and $\lambda=\lambda_1$ can be obtained. Here, we have used the above generalized DT one time and also utilized the identity $\boldsymbol{\Gamma}_1^{[1]}\boldsymbol{T}_1[1]\boldsymbol{\Psi}_1^{[0]}=0$. Then the second-step generalized DT holds

$$\boldsymbol{\Psi}[2]=\boldsymbol{D}[2]\boldsymbol{D}[1]\boldsymbol{\Psi},\quad(12)$$

$$\boldsymbol{T}[2] = \lambda \boldsymbol{I} - \boldsymbol{H}[1]\boldsymbol{\Lambda}_1\boldsymbol{H}[1]^{-1}$$
$$= (\lambda - \lambda_1^*)\boldsymbol{I} + (\lambda_1^* - \lambda_1)\frac{\boldsymbol{\Psi}_1[1]\boldsymbol{\Psi}_1[1]^\dagger}{\boldsymbol{\Psi}_1[1]^\dagger\boldsymbol{\Psi}_1[1]}, \quad (13)$$

$$q_1[2] = \mathrm{e}^{2\eta_1^{[2]}}(q_1[1] + \frac{2\mathrm{i}(\lambda_1^* - \lambda_1)\psi_1[1]\phi_1[1]^*}{\boldsymbol{\Omega}_2}), \quad (14)$$

$$q_2[2] = \mathrm{e}^{2\eta_1^{[2]}}(q_2[1] + \frac{2\mathrm{i}(\lambda_1^* - \lambda_1)\psi_1[1]\chi_1[1]^*}{\boldsymbol{\Omega}_2}), \quad (15)$$

where

$$\boldsymbol{\Psi}_1[1] = (\psi_1[1], \phi_1[1], \chi_1[1])^{\mathrm{T}},$$
$$\boldsymbol{T}_1[1] = \boldsymbol{T}[1]|_{\lambda=\lambda_1} = \lambda_1\boldsymbol{I} - \boldsymbol{H}[0]\boldsymbol{\Lambda}_1\boldsymbol{H}[0]^{-1},$$

and

$$\boldsymbol{\Gamma}_1^{[2]} = \begin{pmatrix} \mathrm{e}^{\eta_1^{[2]}} & & \\ & \mathrm{e}^{-\eta_1^{[2]}} & \\ & & \mathrm{e}^{-\eta_1^{[2]}} \end{pmatrix},$$
$$\boldsymbol{H}[1] = \begin{pmatrix} \psi_1[1] & \phi_1[1]^* & \chi_1[1]^* \\ \phi_1[1] & -\psi_1[1]^* & 0 \\ \chi_1[1] & 0 & -\psi_1[1]^* \end{pmatrix},$$
$$\boldsymbol{\Omega}_2 = |\psi_1[1]|^2 + |\phi_1[1]|^2 + |\chi_1[1]|^2,$$
$$\eta_1^{[2]} = \int (\lambda_1 - \lambda_1^*)\,\boldsymbol{\Omega}_2^{-2}\boldsymbol{\Delta}_2\,\mathrm{d}x,$$
$$\boldsymbol{\Delta}_2 = \rho_1[\,(q_1[1]\phi_1[1]\psi_1[1]^* + q_1[1]^*\phi_1[1]^*\psi_1[1])\,\boldsymbol{\Omega}_2 + 2\mathrm{i}(\lambda_1^* - \lambda_1)|\psi_1[1]|^2|\phi_1[1]|^2] + \rho_2[\,(q_2[1]\chi_1[1]\psi_1[1]^* + q_2[1]^*\chi_1[1]^*\psi_1[1])\,\boldsymbol{\Omega}_2 + 2\mathrm{i}(\lambda_1^* - \lambda_1)|\psi_1[1]|^2|\chi_1[1]|^2].$$

(iii) The third-step generalized DT.

In a similar way, by using the following limit

$$\lim_{\delta\to 0}\frac{\boldsymbol{D}[2]\boldsymbol{D}[1]|_{\lambda=\lambda_1+\delta}\boldsymbol{\Psi}_1}{\delta^2} = \lim_{\delta\to 0}\frac{\boldsymbol{\Gamma}_1^{[2]}(\delta + \boldsymbol{T}_1[2])\boldsymbol{\Gamma}_1^{[1]}(\delta + \boldsymbol{T}_1[1])\boldsymbol{\Psi}_1}{\delta^2}$$
$$= \boldsymbol{\Gamma}_1^{[2]}\boldsymbol{\Gamma}_1^{[1]}\boldsymbol{\Psi}_1^{[0]} + (\boldsymbol{\Gamma}_1^{[2]}\boldsymbol{D}_1[1] + \boldsymbol{D}_1[2]\boldsymbol{\Gamma}_1^{[1]})\boldsymbol{\Psi}_1^{[1]} + \boldsymbol{D}_1[2]\boldsymbol{D}_1[1]\boldsymbol{\Psi}_1^{[2]} \equiv \boldsymbol{\Psi}_1[2], \quad (16)$$

the special vector solution of the Lax pair (2) with $q_1 = q_1[2]$, $q_2 = q_2[2]$, $\lambda = \lambda_1$ can be derived. Besides, the following two identities

$$\boldsymbol{D}_1[1]\boldsymbol{\Psi}_1^{[0]} = 0, \quad \boldsymbol{D}_1[2]\boldsymbol{\Psi}_1[1] = 0,$$

have been applied in the above process. Then the third-step generalized DT can be obtained as

$$\boldsymbol{\Psi}[3] = \boldsymbol{D}[3]\boldsymbol{D}[2]\boldsymbol{D}[1]\boldsymbol{\Psi}, \quad (17)$$
$$\boldsymbol{T}[3] = \lambda\boldsymbol{I} - \boldsymbol{H}[2]\boldsymbol{\Lambda}_1\boldsymbol{H}[2]^{-1}$$
$$= (\lambda - \lambda_1^*)\boldsymbol{I} + (\lambda_1^* - \lambda_1)\frac{\boldsymbol{\Psi}_1[2]\boldsymbol{\Psi}_1[2]^\dagger}{\boldsymbol{\Psi}_1[2]^\dagger\boldsymbol{\Psi}_1[2]}, \quad (18)$$

$$q_1[3] = \mathrm{e}^{2\eta_1^{[3]}}(q_1[2] + \frac{2\mathrm{i}(\lambda_1^* - \lambda_1)\psi_1[2]\phi_1[2]^*}{\boldsymbol{\Omega}_3}), \quad (19)$$

$$q_2[3] = \mathrm{e}^{2\eta_1^{[3]}}(q_2[2] + \frac{2\mathrm{i}(\lambda_1^* - \lambda_1)\psi_1[2]\chi_1[2]^*}{\boldsymbol{\Omega}_3}), \quad (20)$$

where $\boldsymbol{\Psi}_1[2] = (\psi_1[2], \phi_1[2], \chi_1[2])^{\mathrm{T}}$ and $\boldsymbol{T}_1[2] = \boldsymbol{T}[2]|_{\lambda=\lambda_1} = \lambda_1\boldsymbol{I} - \boldsymbol{H}[1]\boldsymbol{\Lambda}_1\boldsymbol{H}[1]^{-1}$,

$$\boldsymbol{\Gamma}_1^{[3]} = \begin{pmatrix} \mathrm{e}^{\eta_1^{[3]}} & & \\ & \mathrm{e}^{-\eta_1^{[3]}} & \\ & & \mathrm{e}^{-\eta_1^{[3]}} \end{pmatrix},$$
$$\boldsymbol{H}[2] = \begin{pmatrix} \psi_1[2] & \phi_1[2]^* & \chi_1[2]^* \\ \phi_1[2] & -\psi_1[2]^* & 0 \\ \chi_1[2] & 0 & -\psi_1[2]^* \end{pmatrix},$$
$$\boldsymbol{\Omega}_3 = |\psi_1[2]|^2 + |\phi_1[2]|^2 + |\chi_1[2]|^2,$$
$$\eta_1^{[3]} = \int (\lambda_1 - \lambda_1^*)\,\boldsymbol{\Omega}_3^{-2}\boldsymbol{\Delta}_3\,\mathrm{d}x,$$
$$\boldsymbol{\Delta}_3 = \rho_1[\,(q_1[2]\phi_1[2]\psi_1[2]^* + q_1[2]^*\phi_1[2]^*\psi_1[2])\,\boldsymbol{\Omega}_3 + 2\mathrm{i}(\lambda_1^* - \lambda_1)|\psi_1[2]|^2|\phi_1[2]|^2] + \rho_2[\,(q_2[2]\chi_1[2]\psi_1[2]^* + q_2[2]^*\chi_1[2]^*\psi_1[2])\,\boldsymbol{\Omega}_3 + 2\mathrm{i}(\lambda_1^* - \lambda_1)|\psi_1[2]|^2|\chi_1[2]|^2].$$

(iv) The fourth-step generalized DT.

In addition, the special vector solution of the Lax pair (2) with $q_1 = q_1[3]$, $q_2 = q_2[3]$, and $\lambda = \lambda_1$ can be presented as follows:

$$\lim_{\delta\to 0}\frac{\boldsymbol{D}[3]\boldsymbol{D}[2]\boldsymbol{D}[1]|_{\lambda=\lambda_1+\delta}\boldsymbol{\Psi}_1}{\delta^3} = \lim_{\delta\to 0}\frac{\boldsymbol{\Gamma}_1^{[3]}(\delta + \boldsymbol{T}_1[3])\boldsymbol{\Gamma}_1^{[2]}(\delta + \boldsymbol{T}_1[2])\boldsymbol{\Gamma}_1^{[1]}(\delta + \boldsymbol{T}_1[1])}{\delta^3}$$
$$= \boldsymbol{\Gamma}_1^{[3]}\boldsymbol{\Gamma}_1^{[2]}\boldsymbol{\Gamma}_2^{[1]}\boldsymbol{\Psi}_1^{[0]} + (\,\boldsymbol{\Gamma}_1^{[3]}\boldsymbol{\Gamma}_1^{[2]}\boldsymbol{D}_1[1] + \boldsymbol{\Gamma}_1^{[3]}\boldsymbol{D}_1[2]\boldsymbol{\Gamma}_1^{[1]} + \boldsymbol{D}_1[3]\boldsymbol{\Gamma}_1^{[2]}\boldsymbol{\Gamma}_1^{[1]}\,)\boldsymbol{\Psi}_1^{[1]}$$
$$+ (\boldsymbol{D}_1[3]\boldsymbol{\Gamma}_1^{[2]}\boldsymbol{D}_1[1] + \boldsymbol{D}_1[3]\boldsymbol{D}_1[2]\boldsymbol{\Gamma}_1^{[1]})\Psi_1^{[2]} + \boldsymbol{D}_1[3]\boldsymbol{D}_1[2]\boldsymbol{D}_1[1]\boldsymbol{\Psi}_1^{[3]} \equiv \boldsymbol{\Psi}_1[3], \quad (21)$$

by using the following three identities

$$\boldsymbol{D}_1[1]\boldsymbol{\Psi}_1^{[0]}=0,\quad \boldsymbol{D}_1[2]\boldsymbol{\Psi}_1[1]=0,\quad \boldsymbol{D}_1[3]\boldsymbol{\Psi}_1[2]=0.$$

Continuing the above process, we can construct the fourth-step generalized DT as follows:

$$\boldsymbol{\Psi}[4]=\boldsymbol{D}[4]\boldsymbol{D}[3]\boldsymbol{D}[2]\boldsymbol{D}[1]\boldsymbol{\Psi}, \tag{22}$$

$$\begin{aligned}\boldsymbol{T}[4]&=\lambda\boldsymbol{I}-\boldsymbol{H}[3]\boldsymbol{\Lambda}_1\boldsymbol{H}[3]^{-1}\\&=(\lambda-\lambda_1^*)\boldsymbol{I}+(\lambda_1^*-\lambda_1)\frac{\boldsymbol{\Psi}_1[3]\boldsymbol{\Psi}_1[3]^{\dagger}}{\boldsymbol{\Psi}_1[3]^{\dagger}\boldsymbol{\Psi}_1[3]},\end{aligned} \tag{23}$$

$$q_1[4]=\mathrm{e}^{2\eta_1^{[4]}}\Big(q_1[3]+\frac{2\mathrm{i}(\lambda_1^*-\lambda_1)\psi_1[3]\phi_1[3]^*}{\boldsymbol{\Omega}_4}\Big), \tag{24}$$

$$q_2[4]=\mathrm{e}^{2\eta_1^{[4]}}\Big(q_2[3]+\frac{2i(\lambda_1^*-\lambda_1)\psi_1[3]\chi_1[3]^*}{\boldsymbol{\Omega}_4}\Big), \tag{25}$$

where $\boldsymbol{\Psi}_1[3]=(\psi_1[3],\phi_1[3],\chi_1[3])^{\mathrm{T}}$, and $\boldsymbol{T}_1[3]=\boldsymbol{T}[3]|_{\lambda=\lambda_1}=\lambda_1\boldsymbol{I}-\boldsymbol{H}[2]\boldsymbol{\Lambda}_1\boldsymbol{H}[2]^{-1}$,

$$\boldsymbol{\Gamma}_1^{[4]}=\begin{pmatrix}\mathrm{e}^{\eta_1^{[4]}}&&\\&\mathrm{e}^{-\eta_1^{[4]}}&\\&&\mathrm{e}^{-\eta_1^{[4]}}\end{pmatrix},$$

$$\boldsymbol{H}[3]=\begin{pmatrix}\psi_1[3]&\phi_1[3]^*&\chi_1[3]^*\\\phi_1[3]&-\psi_1[3]^*&0\\\chi_1[3]&0&-\psi_1[3]^*\end{pmatrix},$$

$$\boldsymbol{\Omega}_4=|\psi_1[3]|^2+|\phi_1[3]|^2+|\chi_1[3]|^2,$$

$$\eta_1^{[4]}=\int(\lambda_1-\lambda_1^*)\boldsymbol{\Omega}_4^{-2}\Delta_4\,\mathrm{d}x,$$

$$\begin{aligned}\boldsymbol{\Delta}_4=\rho_1[&(q_1[3]\phi_1[3]\psi_1[3]^*+q_1[3]^*\phi_1[3]^*\psi_1[3])\boldsymbol{\Omega}_4\\&+2\mathrm{i}(\lambda_1^*-\lambda_1)|\psi_1[3]|^2|\phi_1[3]|^2]+\rho_2[(q_2[3]\chi_1[3]\psi_1[3]^*\\&+q_2[3]^*\chi_1[3]^*\psi_1[3])\boldsymbol{\Omega}_4+2\mathrm{i}(\lambda_1^*-\lambda_1)|\psi_1[3]|^2|\chi_1[3]|^2].\end{aligned}$$

Owing to the complexity and irregularity of the expressions of $\boldsymbol{\Psi}_1[j]$, such as Eqs. (16) and (21), the unified formula of the N-step generalized DT of the CCQNLS equations cannot be given easily. Combining the special vector solution of the Lax pair (2) and the higher-order generalized DT, we can obtain the corresponding higher-order localized wave solutions consisting of higher-order rogue wave, higher-order rogue wave interacting with multi-soliton or multi-breather.

3. Nonlinear localized wave solutions

In this section, some nonlinear localized wave solutions[31] of the CCQNLS equations (1) are constructed through the above generalized DT. Here, the first- and second-order localized waves are discussed in detail and some figures of these kinds of localized wave solutions are also exhibited. Besides, some dynamic structures of these nonlinear waves are demonstrated.

3.1. The first-order localized wave solutions

In the following, we choose a nontrivial seed solution of the CCQNLS equations (1)

$$q_1[0]=d_1\mathrm{e}^{\mathrm{i}\theta},\qquad q_2[0]=d_2\mathrm{e}^{\mathrm{i}\theta}, \tag{26}$$

where $\theta=[(\rho_1d_1^2+\rho_2d_2^2)^2+2(d_1^2+d_2^2)]t$, d_1 and d_2 are all real constants ($d_1\neq d_2$). For convenience, the above seed solutions are chosen periodically in time variable t without depending on space variable x. Choosing $q_1=q_1[0]$, $q_2=q_2[0]$, the special vector solutions of the Lax pair (2) can be elaborately expressed as

$$\boldsymbol{\Psi}_1=\begin{pmatrix}(c_1\mathrm{e}^{M_1}-c_2\mathrm{e}^{-M_1})\mathrm{e}^{\mathrm{i}\theta/2}\\r_1(c_1\mathrm{e}^{-M_1}-c_2\mathrm{e}^{M_1})\mathrm{e}^{-\mathrm{i}\theta/2}-\alpha d_2\mathrm{e}^{M_2}\\r_2(c_1\mathrm{e}^{-M_1}-c_2\mathrm{e}^{M_1})\mathrm{e}^{-\mathrm{i}\theta/2}+\alpha d_1\mathrm{e}^{M_2}\end{pmatrix}, \tag{27}$$

where

$$c_1=\frac{\Big[(2\lambda-\rho_1d_1^2-\rho_2d_2^2)-\sqrt{(2\lambda-\rho_1d_1^2-\rho_2d_2^2)^2+4(d_1^2+d_2^2)}\,\Big]^{1/2}}{\sqrt{(2\lambda-\rho_1d_1^2-\rho_2d_2^2)^2+4(d_1^2+d_2^2)}},$$

$$c_2=\frac{\Big[(2\lambda-\rho_1d_1^2-\rho_2d_2^2)+\sqrt{(2\lambda-\rho_1d_1^2-\rho_2d_2^2)^2+4(d_1^2+d_2^2)}\,\Big]^{1/2}}{\sqrt{(2\lambda-\rho_1d_1^2-\rho_2d_2^2)^2+4(d_1^2+d_2^2)}},$$

$$r_1=\frac{d_1}{\sqrt{d_1^2+d_2^2}},\quad r_2=\frac{d_2}{\sqrt{d_1^2+d_2^2}},\quad s_k=m_k+in_k\ (1\leqslant k\leqslant N),$$

$$M_1=\frac{\mathrm{i}}{2}\sqrt{(2\lambda-\rho_1d_1^2-\rho_2d_2^2)^2+4(d_1^2+d_2^2)}\Big[x+(2\lambda+\rho_1d_1^2+\rho_2d_2^2)t+\sum_{k=1}^{N}s_k\varepsilon^{2k}\Big],$$

$$M_2=\frac{\mathrm{i}}{2}[(2\lambda-\rho_1d_1^2-\rho_2d_2^2)x+(4\lambda^2-2(\rho_1d_1^2+\rho_2d_2^2)^2)t],$$

here, m_k, n_k, and α are all real free parameters. Choosing the spectral parameter $\lambda=(1/2)(\rho_1d_1^2+\rho_2d_2^2)+\mathrm{i}\sqrt{d_1^2+d_2^2}+\varepsilon^2$ with a small real parameter ε, the Taylor expansion of the above vector function $\boldsymbol{\Psi}_1$ at $\varepsilon=0$ can be derived as

$$\boldsymbol{\Psi}_1(\varepsilon)=\boldsymbol{\Psi}_1^{[0]}+\boldsymbol{\Psi}_1^{[1]}\varepsilon^2+\boldsymbol{\Psi}_1^{[2]}\varepsilon^4+\boldsymbol{\Psi}_1^{[3]}\varepsilon^6+\cdots+\boldsymbol{\Psi}_1^{[l]}\varepsilon^{2l}+\cdots, \tag{28}$$

where

$$\boldsymbol{\Psi}_1^{[l]} = (\psi_1^{[l]}, \phi_1^{[l]}, \chi_1^{[l]})^{\mathrm{T}} = \frac{\partial^{2l}\boldsymbol{\Psi}_1}{(2l)!\partial\varepsilon^{2l}}\bigg|_{\varepsilon=0} \quad (l = 0, 1, 2, 3, \ldots),$$

and

$$\begin{aligned}
\psi_1^{[0]} &= \frac{(-1+\mathrm{i})[4\sqrt{d_1^2+d_2^2}(\rho_1 d_1^2+\rho_2 d_2^2)t+4\mathrm{i}(d_1^2+d_2^2)t+2\sqrt{d_1^2+d_2^2}x+1]\,\mathrm{e}^{\mathrm{i}\theta/2}}{2(d_1^2+d_2^2)^{1/4}},\\
\phi_1^{[0]} &= \frac{(1-\mathrm{i})d_1[4\sqrt{d_1^2+d_2^2}(\rho_1 d_1^2+\rho_2 d_1^2)t+4\mathrm{i}(d_1^2+d_2^2)t+2\sqrt{d_1^2+d_2^2}x-1]\,\mathrm{e}^{-\mathrm{i}\theta/2}}{2(d_1^2+d_1^2)^{3/4}} - \alpha d_2\,\mathrm{e}^{\xi},\\
\chi_1^{[0]} &= \frac{(1-\mathrm{i})d_2[4\sqrt{d_1^2+d_2^2}(\rho_1 d_1^2+\rho_2 d_1^2)t+4\mathrm{i}(d_1^2+d_2^2)t+2\sqrt{d_1^2+d_2^2}x-1]\,\mathrm{e}^{-\mathrm{i}\theta/2}}{2(d_1^2+d_1^2)^{3/4}} + \alpha d_1\,\mathrm{e}^{\xi},\\
\psi_1^{[1]} &= G\mathrm{e}^{\mathrm{i}\theta/2},\\
\phi_1^{[1]} &= \frac{d_1}{\sqrt{d_1^2+d_2^2}}\left[-G+(1+\mathrm{i})(d_1^2+d_2^2)^{1/4}\left(x+2\left(\rho_1 d_1^2+\rho_2 d_2^2+\mathrm{i}\sqrt{d_1^2+d_2^2}\right)t\right)^2-\frac{1+\mathrm{i}}{4(d_1^2+d_2^2)^{3/4}}\right]\mathrm{e}^{-\mathrm{i}\theta/2}\\
&\quad -\mathrm{i}\alpha d_2\left[x+2\left(\rho_1 d_1^2+\rho_2 d_2^2+2\mathrm{i}\sqrt{d_1^2+d_2^2}\right)t\right]\mathrm{e}^{\xi},\\
\chi_1^{[1]} &= \frac{d_2}{\sqrt{d_1^2+d_2^2}}\left[-G+(1+\mathrm{i})(d_1^2+d_2^2)^{1/4}\left(x+2\left(\rho_1 d_1^2+\rho_2 d_2^2+\mathrm{i}\sqrt{d_1^2+d_2^2}\right)t\right)^2-\frac{1+\mathrm{i}}{4(d_1^2+d_2^2)^{3/4}}\right]\mathrm{e}^{-\mathrm{i}\theta/2}\\
&\quad +\mathrm{i}\alpha d_1\left[x+2\left(\rho_1 d_1^2+\rho_2 d_2^2+2\mathrm{i}\sqrt{d_1^2+d_2^2}\right)t\right]\mathrm{e}^{\xi},\\
&\cdots
\end{aligned}$$

with

$$\begin{aligned}
\xi &= -\sqrt{d_1^2+d_2^2}x-\left[\frac{\mathrm{i}}{2}(\rho_1 d_1^2+\rho_2 d_2^2)^2+2\sqrt{d_1^2+d_2^2}(\rho_1 d_1^2+\rho_2 d_2^2)+2\mathrm{i}(d_1^2+d_2^2)\right]t,\\
G &= \frac{1}{3}(1+\mathrm{i})(d_1^2+d_2^2)^{3/4}\left[x+2\left(\rho_1 d_1^2+\rho_2 d_2^2+\mathrm{i}\sqrt{d_1^2+d_2^2}\right)t\right]^3+\frac{1}{2}(1+\mathrm{i})(d_1^2+d_2^2)^{1/4}\\
&\quad\cdot\left[x+2\left(\rho_1 d_1^2+\rho_2 d_2^2+\mathrm{i}\sqrt{d_1^2+d_2^2}\right)t\right]^2+\frac{1+\mathrm{i}}{4(d_1^2+d_2^2)^{1/4}}\left[x+2\left(\rho_1 d_1^2+\rho_2 d_2^2+\mathrm{i}\sqrt{d_1^2+d_2^2}\right)t\right]\\
&\quad+(-1+\mathrm{i})(d_1^2+d_2^2)^{1/4}(2t+m_1+\mathrm{i}n_1)-\frac{1+\mathrm{i}}{8(d_1^2+d_2^2)^{3/4}}.
\end{aligned}$$

It can be found that the vector function $\boldsymbol{\Psi}_1^{[0]}$ is a solution of the Lax pair (2) at $q_1 = q_1[0]$, $q_2 = q_2[0]$, and $\lambda = \lambda_1 = (1/2)(\rho_1 d_1^2 + \rho_2 d_2^2) + \mathrm{i}\sqrt{d_1^2+d_2^2}$. Through the first-step generalized DT (8)–(10), we can gain the first-order localized wave solutions of the CCQNLS system (1). Owing to the complicated integral operation existing in $\eta_1^{[1]}$, we choose to obtain the expressions of the first-order semi-rational solutions of Eq. (1) after fixing the values of the free parameters. According to different values of the free parameters α, d_1, and d_2, we can obtain three types of the first-order nonlinear localized waves in the CCQNLS equations.[31,32]

i) When $\alpha = 0$, in order to gain the nontrivial solutions of Eq. (1), we set that d_1 and d_2 are all not zero, hereby, the components q_1 and q_2 are proportional to each other. Here, the first-order semi-rational solutions degenerate to the rational ones and we can obviously find they are the first-order rogue waves, see Fig. 1. Choosing $d_1 = 1$, $d_2 = -2$, $\rho_1 = 1/10$, and $\rho_2 = 1/20$, the expression of the first-order rogue wave solutions of Eq. (1) can be written as

$$q_1[1] = \frac{400\mathrm{i}t - 2036t^2 - 120tx - 100x^2 + 15}{2036t^2 + 120tx + 100x^2 + 5}\exp\left[\frac{\mathrm{i}(2054324t^3 + 121080t^2x + 100900tx^2 + 5765t + 1200x)}{100(2036t^2 + 120tx + 100x^2 + 5)}\right], \tag{29}$$

$$q_2[1] = -2\frac{400\mathrm{i}t - 2036t^2 - 120tx - 100x^2 + 15}{2036t^2 + 120tx + 100x^2 + 5}\exp\left[\frac{\mathrm{i}(2054324t^3 + 121080t^2x + 100900tx^2 + 5765t + 1200x)}{100(2036t^2 + 120tx + 100x^2 + 5)}\right]. \tag{30}$$

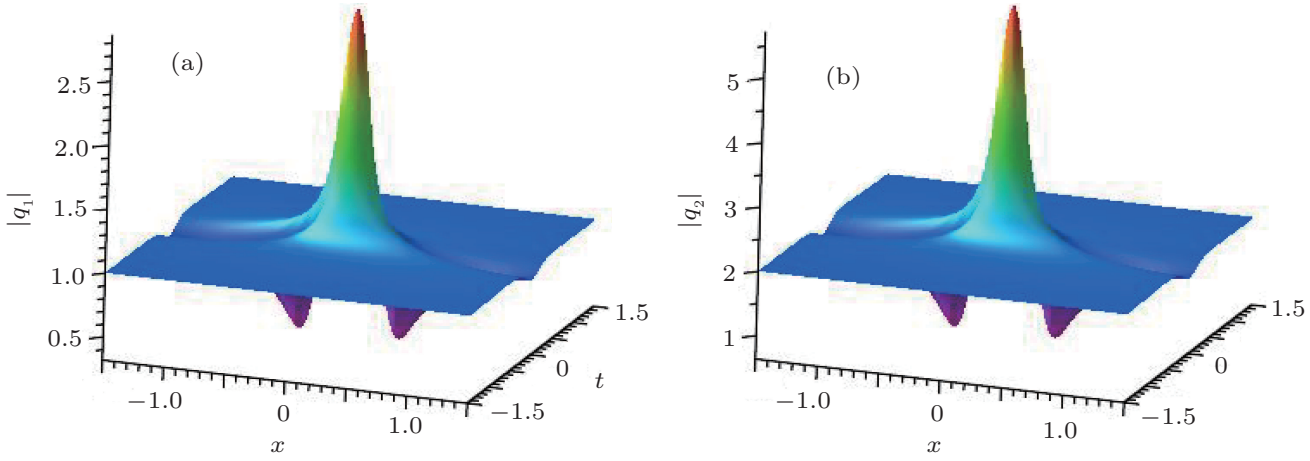


Fig. 1. (color online) Evolution plot of the first-order rogue wave in the CCQNLS: (a) q_1,(b)q_2.

ii) Setting one of the two free parameters d_1 and d_2 is zero and $\alpha \neq 0$, we can obtain the first kind of the second-order semi-rational solutions that a first-order rogue wave interacting with a bright soliton and a dark soliton respectively in the two components q_1 and q_2. Choosing $d_1 = 0$, $d_2 = 1$, $\rho_1 = 1/10$, and $\rho_2 = 1/20$, the first kind of the first-order semi-rational solution of Eq. (1) can be expressed as

$$q_1[1] = \frac{2\alpha[(19/5)\mathrm{i}t + (21/5)t - 2\mathrm{i}x + 2x + 1 - \mathrm{i}]\,\mathrm{e}^{\xi_1}}{(401/25)t^2 + (4/5)tx + 4x^2 + 1 + \alpha^2\,\mathrm{e}^{-1/5t-2x}}, \tag{31}$$

$$q_2[1] = \left\{1 + \frac{2[1 - (401/25)t^2 - (4/5)tx + 8\mathrm{i}t - 4x^2]}{(401/25)t^2 + (4/5)tx + 4x^2 + 1 + \alpha^2\,\mathrm{e}^{-1/5t-2x}}\right\}\mathrm{e}^{\xi_2}, \tag{32}$$

where

$$\begin{aligned}\xi_1 = {} & \frac{1}{400(25\alpha^2\,\mathrm{e}^{-(1/5)t-2x} + 401t^2 + 20tx + 100x^2 + 25)}\Big\{\left[(30025\mathrm{i} - 1000)\alpha^2 t - 10000\alpha^2 x - 3000\mathrm{i}\alpha^2\right]\mathrm{e}^{-(1/5)t-2x} \\ & + 481601\mathrm{i}t^3 + 24020\mathrm{i}t^2x + 120100\mathrm{i}tx^2 - 16040t^3 - 161200xt^2 - 12000x^2t - 40000x^3 \\ & + (30425\mathrm{i} - 1000)t + (4000\mathrm{i} - 10000)x\Big\},\end{aligned}$$

$$\begin{aligned}\xi_2 = {} & \frac{1}{400(25\alpha^2\,\mathrm{e}^{-(1/5)t-2x} + 401t^2 + 20tx + 100x^2 + 25)}\Big[(20025\alpha^2 t - 3000\alpha^2)\,\mathrm{e}^{-(1/5)t-2x} \\ & + 321201t^3 + 16020xt^2 + 80100x^2t + 20425t + 4000x\Big].\end{aligned}$$

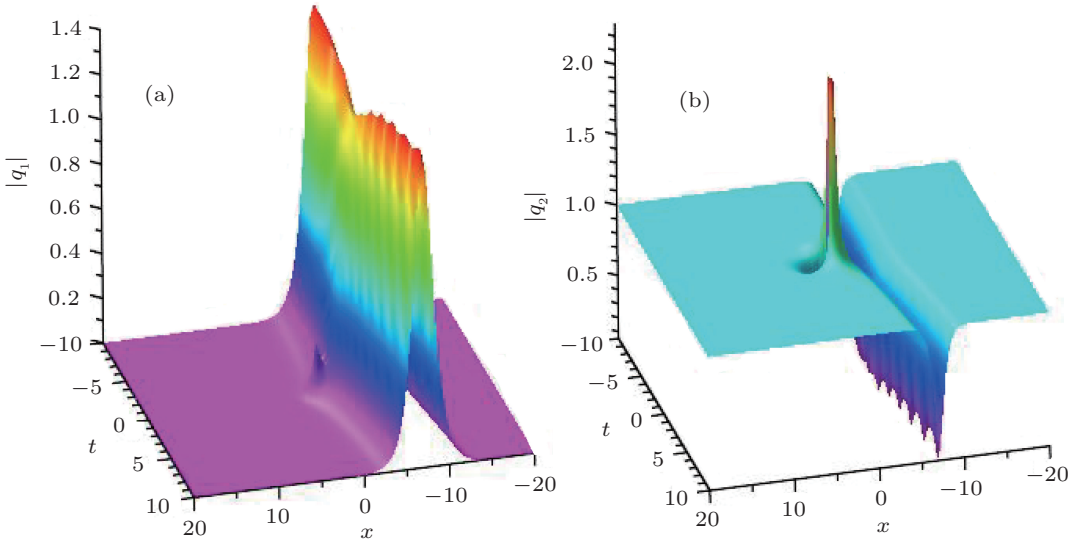


Fig. 2. (color online) Evolution plot of the interactional solution between the first-order rogue wave and one-soliton in the CCQNLS equations with the parameters chosen by $\alpha = 1/10$. (a) A first-order rogue wave and a bright soliton separate in q_1 component; (b) a first-order rogue wave and a dark soliton separate in q_2 component.

Here, the interesting interactional phenomenon can be demonstrated in Figs. 2 and 3. Moreover, by decreasing the absolute value of α, it can be shown that a first-order rogue wave and a bright (dark) soliton separate in Fig. 2. While increasing the

absolute value of α, it demonstrates the first-order rogue wave merges with one soliton in Fig. 3. We notice that in Fig. 2(b), a dark soliton and a rogue wave emerge on the distribution of the spacial-temporal structure, and the amplitude of the rogue wave is about three times greater than the height of the background. However, when the bright soliton and the rogue wave divide in Fig. 2(a), we can find that the rogue wave cannot be easily identified. At this time, the amplitude of the plane wave background in q_1 component is zero and the amplitude of the rogue wave is dependent on this background, so the rogue wave is not observed easily.

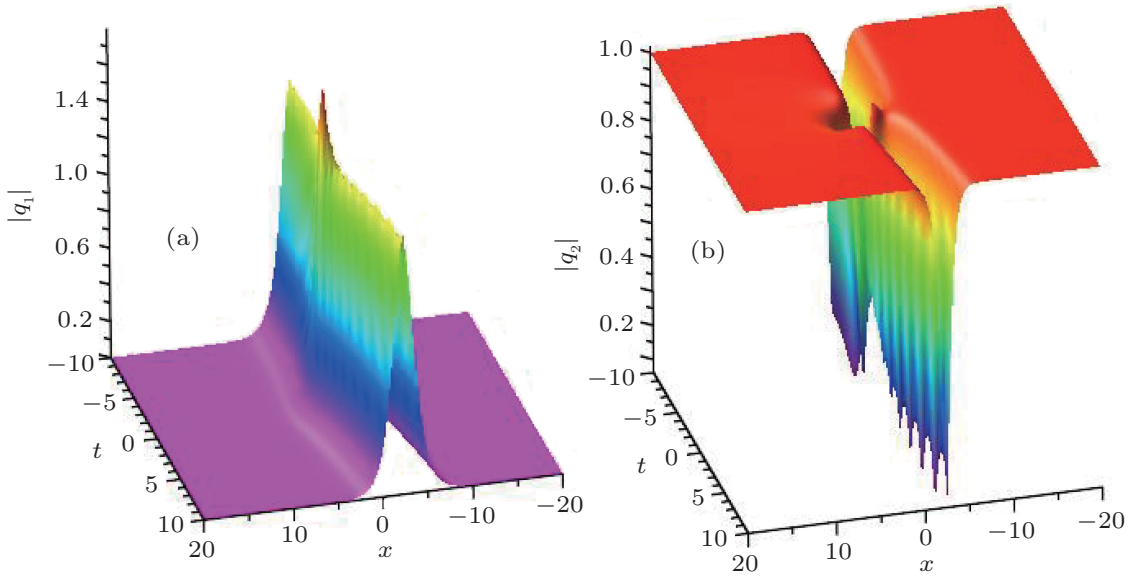


Fig. 3. (color online) Evolution plot of the interactional solution between the first-order rogue wave and one-soliton in the CCQNLS equations with the parameters chosen by $\alpha = 10$. (a) A first-order rogue wave merges with a bright soliton in q_1 component; (b) a first-order rogue wave merges with a dark soliton in q_2 component.

iii) Setting $d_1 \neq 0$, $d_2 \neq 0$, and $\alpha \neq 0$, the second kind of the first-order semi-rational solutions consisting of one first-order rogue wave and one breather can be generated in both q_1 and q_2 components. Choosing $d_1 = 1$, $d_2 = -2$, $\rho_1 = 1/10$, and $\rho_2 = 1/20$, the second kind of the first-order semi-rational solution of Eq. (1) can be written as

$$q_1[1] = \frac{F_1 \exp\left[\left(\frac{1609}{400}\right)\mathrm{i}t\right] + F_2 \exp\left[\left(\frac{2409}{400}\right)\mathrm{i}t - \sqrt{2}x - \frac{3}{10}\sqrt{2}t\right] + 50\sqrt{2}\alpha^2 \exp\left[\left(\frac{1609}{400}\right)\mathrm{i}t - \frac{3}{5}\sqrt{2}t - 2\sqrt{2}x\right]}{1618t^2 + 120xt + 200x^2 + 25 + 50\sqrt{2}\alpha^2 \exp\left[-\frac{\sqrt{2}}{5}(3t + 10x)\right]} \mathrm{e}^{2\xi_3}, \quad (33)$$

$$q_2[1] = \frac{F_1 \exp\left[\left(\frac{1609}{400}\right)\mathrm{i}t\right] - F_2 \exp\left[\left(\frac{2409}{400}\right)\mathrm{i}t - \sqrt{2}x - \frac{3}{10}\sqrt{2}t\right] + 50\sqrt{2}\alpha^2 \exp\left[\left(\frac{1609}{400}\right)\mathrm{i}t - \frac{3}{5}\sqrt{2}t - 2\sqrt{2}x\right]}{1618t^2 + 120xt + 200x^2 + 25 + 50\sqrt{2}\alpha^2 \exp\left[-\left(\frac{\sqrt{2}}{5}\right)(3t + 10x)\right]} \mathrm{e}^{2\xi_3}, \quad (34)$$

where

$$F_1 = 800\mathrm{i}t - 1618t^2 - 120tx - 200x^2 + 75,$$

$$F_2 = \frac{100}{809}2^{1/4}\alpha(20\mathrm{i}\sqrt{2} + 20\sqrt{2} + 3 - 3\mathrm{i})(400\mathrm{i}\sqrt{2}x - 15\sqrt{2} + 200\mathrm{i} - 1618t - 60x),$$

$$\xi_3 = \frac{1}{40(50\sqrt{2}\alpha^2 \exp[-(\sqrt{2}/5)(3t + 10x)] + 1618t^2 + 120tx + 200x^2 + 25)}\left[\frac{5}{809}2^{1/4}\alpha(3\mathrm{i}\sqrt{2} + 3\sqrt{2} - 40 + 40\mathrm{i})\right.$$
$$\cdot(400\mathrm{i}\sqrt{2}x + 15\sqrt{2} - 200\mathrm{i} - 1618t - 60x)\exp[-(3\sqrt{2}/10)t - \sqrt{2}x + 2\mathrm{i}t] - \frac{5}{809}2^{1/4}\alpha(3\mathrm{i}\sqrt{2} - 3\sqrt{2} + 40 + 40\mathrm{i})(400\mathrm{i}\sqrt{2}x$$
$$- 15\sqrt{2} - 200\mathrm{i} + 1618t + 60x)\exp\left[-(3/10)\sqrt{2}t - \sqrt{2}x - 2\mathrm{i}t\right] - \frac{3}{1618}\mathrm{i}\sqrt{2}(400\mathrm{i}\sqrt{2}x - 15\sqrt{2} + 200\mathrm{i} - 1618t - 60x)$$
$$\left.\cdot(400\mathrm{i}\sqrt{2}x + 200\mathrm{i} + 15\sqrt{2} + 1618t + 60x)\right].$$

It is shown that the two components q_1 and q_2 are all the hybrid solutions between one breather and one first-order rogue wave in Figs. 4 and 5. Similarly, by decreasing the absolute value of α, we can observe that the first-order rogue wave and one breather separate in Fig. 4. Meanwhile through increasing the absolute value of α, the first-order rogue wave and one breather merge in Fig. 5.

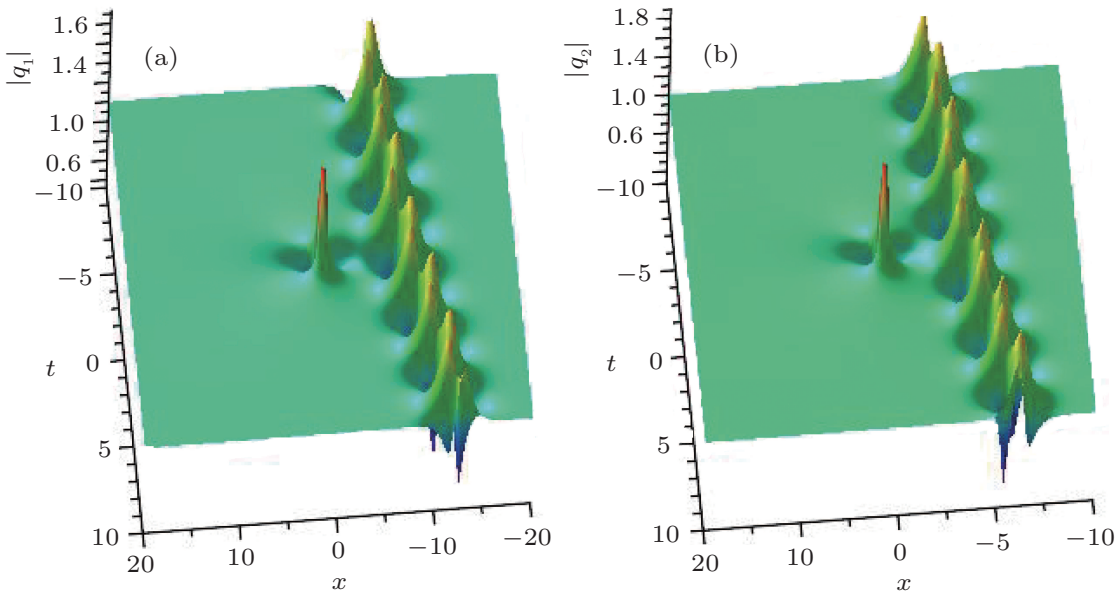


Fig. 4. (color online) Evolution plot of the interactional solution between the first-order rogue wave and one-breather in the CCQNLS equations with the parameters chosen by $\alpha = 10^{-4}$. A first-order rogue wave and a breather separate in the two components: (a) q_1 component,(b) q_2 component.

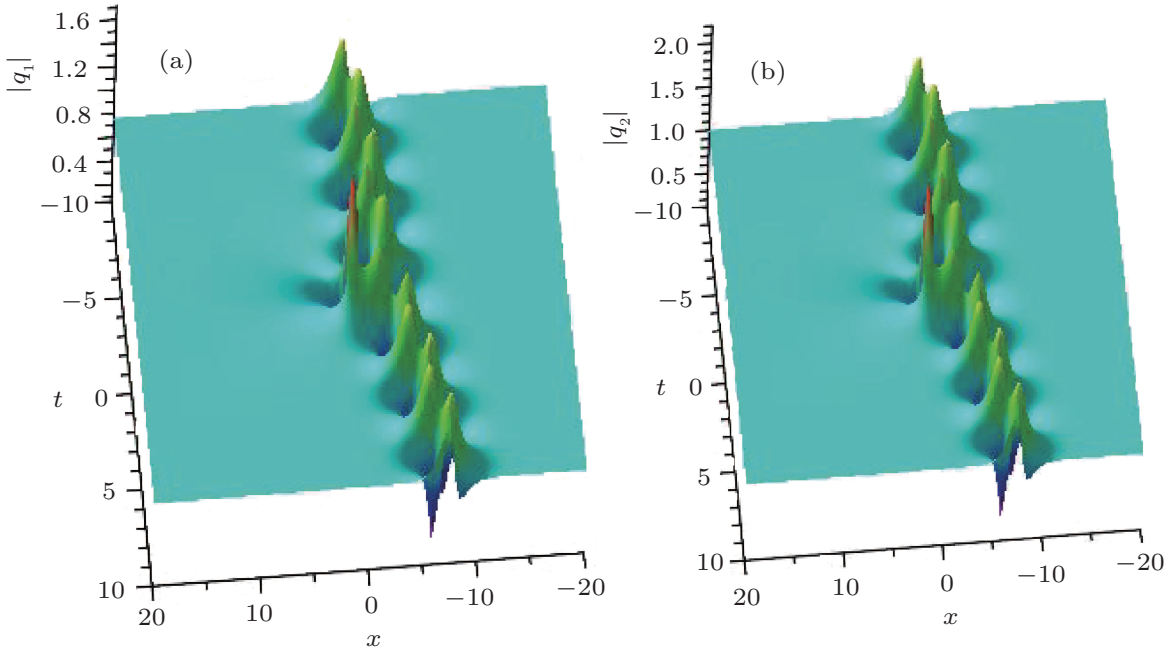


Fig. 5. (color online) Evolution plot of the interactional solution between the first-order rogue wave and one-breather in the CCQNLS equations with the parameters chosen by $\alpha = 1/10$. A first-order rogue wave merges with a breather in the two components: (a) q_1 component, (b) q_2 component.

3.2. The second-order localized wave solutions

In this subsection, we construct the second-order localized wave solutions of the CCQNLS equations (1), which include the second-order rogue wave, two dark (bright) solitons interacting with the second-order rogue wave, and two parallel breathers together with the second-order rogue wave.[32,33]

Considering the following limit

$$\lim_{\varepsilon\to 0}\frac{\boldsymbol{\Gamma}_1^{[1]}\boldsymbol{T}[1]|_{\lambda=\lambda_1+\varepsilon^2}\boldsymbol{\Phi}_1}{\varepsilon^2}=\lim_{\varepsilon\to 0}\frac{\boldsymbol{\Gamma}_1^{[1]}(\varepsilon^2+\boldsymbol{T}_1[1])\boldsymbol{\Phi}_1}{\varepsilon^2}=\boldsymbol{\Gamma}_1^{[1]}(\boldsymbol{\Psi}_1^{[0]}+\boldsymbol{T}_1[1]\boldsymbol{\Psi}_1^{[1]})\equiv\boldsymbol{\Psi}_1[1], \tag{35}$$

where

$$\boldsymbol{T}_1[1]=\lambda_1\boldsymbol{I}-\boldsymbol{H}[0]\boldsymbol{\Lambda}_1\boldsymbol{H}[0]^{-1}=(\lambda_1-\lambda_1^*)\boldsymbol{I}+(\lambda_1^*-\lambda_1)\frac{\boldsymbol{\Psi}_1^{[0]}\boldsymbol{\Psi}_1^{[0]\dagger}}{\boldsymbol{\Psi}_1^{[0]\dagger}\boldsymbol{\Psi}_1^{[0]}}=2\mathrm{i}\sqrt{d_1^2+d_2^2}\Big(\boldsymbol{I}-\frac{\boldsymbol{\Psi}_1^{[0]}\boldsymbol{\Psi}_1^{[0]\dagger}}{\boldsymbol{\Psi}_1^{[0]\dagger}\boldsymbol{\Psi}_1^{[0]}}\Big), \tag{36}$$

a special vector solution $\boldsymbol{\Psi}_1[1]$ is generated through choosing $q_1 = q_1[1]$, $q_2 = q_2[1]$, and $\lambda_1 = (1/2)(\rho_1 d_1^2 + \rho_2 d_2^2) + \mathrm{i}\sqrt{d_1^2 + d_2^2}$ in the Lax pair (2).

Proposition 1 In order to avoid the complicated integral operation in the expression of $\boldsymbol{\Gamma}_1^{[1]}$, we give the expressions of modules of $q_1[2]$ and $q_2[2]$ through Eqs. (8)–(15),

$$|q_1[2]| = \left| q_1[0] + \frac{2\mathrm{i}(\lambda_1^* - \lambda_1)\psi_1[0]\phi_1[0]^*}{|\psi_1[0]|^2 + |\phi_1[0]|^2 + |\chi_1[0]|^2} + \frac{2\mathrm{i}(\lambda_1^* - \lambda_1)\phi_1^{(1)}[1]\phi_1^{(2)*}[1]}{|\phi_1^{(1)}[1]|^2 + |\phi_1^{(2)}[1]|^2 + |\phi_1^{(3)}[1]|^2} \right|, \tag{37}$$

$$|q_2[2]| = \left| q_2[0] + \frac{2\mathrm{i}(\lambda_1^* - \lambda_1)\psi_1[0]\chi_1[0]^*}{|\psi_1[0]|^2 + |\phi_1[0]|^2 + |\chi_1[0]|^2} + \frac{2\mathrm{i}(\lambda_1^* - \lambda_1)\phi_1^{(1)}[1]\phi_1^{(3)*}[1]}{|\phi_1^{(1)}[1]|^2 + |\phi_1^{(2)}[1]|^2 + |\phi_1^{(3)}[1]|^2} \right|, \tag{38}$$

where $\boldsymbol{\Phi}_1[1] = \boldsymbol{\Psi}_1^{[0]} + \boldsymbol{T}_1[1]\boldsymbol{\Psi}_1^{[1]} = (\phi_1^{(1)}[1], \phi_1^{(2)}[1], \phi_1^{(3)}[1])^{\mathrm{T}}$.

Proof From the expressions of $\boldsymbol{\Lambda}_1$ and $\boldsymbol{\Lambda}_2$, we can gain the following equalities

$$\boldsymbol{\Omega}_1 = \rho_1[2\mathrm{Re}(q_1[0]\phi_1[0]\psi_1[0]^*)\boldsymbol{\Omega}_1 + 4\,\mathrm{Im}(\lambda_1)|\psi_1[0]|^2|\phi_1[0]|^2] + \rho_2[2\mathrm{Re}(q_2[0]\chi_1[0]\psi_1[0]^*)\boldsymbol{\Omega}_1 + 4\,\mathrm{Im}(\lambda_1)|\psi_1[0]|^2|\chi_1[0]|^2], \tag{39}$$

$$\boldsymbol{\Omega}_2 = \rho_1[2\mathrm{Re}(q_1[1]\phi_1[1]\psi_1[1]^*)\boldsymbol{\Omega}_2 + 4\,\mathrm{Im}(\lambda_1)|\psi_1[1]|^2|\phi_1[1]|^2] + \rho_2[2\mathrm{Re}(q_2[1]\chi_1[1]\psi_1[1]^*)\boldsymbol{\Omega}_2 + 4\,\mathrm{Im}(\lambda_1)|\psi_1[1]|^2|\chi_1[1]|^2]. \tag{40}$$

Furthermore, it is clear that $\boldsymbol{\Omega}_1$ and $\boldsymbol{\Omega}_2$ are all real functions of x and t through Eqs. (39) and (40). Thus, the expressions of $\eta_1^{[1]}$ and $\eta_1^{[2]}$ can be written as

$$\eta_1^{[1]} = \mathrm{i}\int 2\mathrm{Im}(\lambda_1)\ \boldsymbol{\Omega}_1^{-2}\boldsymbol{\Delta}_1\,\mathrm{d}x,$$

$$\eta_1^{[2]} = \mathrm{i}\int 2\mathrm{Im}(\lambda_1)\ \boldsymbol{\Omega}_2^{-2}\boldsymbol{\Delta}_2\,\mathrm{d}x. \tag{41}$$

Choosing the integration constants in Eq. (41) to be zero, we can find that $\eta_1^{[1]}$ and $\eta_1^{[2]}$ are pure imaginary functions of x and t. Based on the above facts, the two following relations can be obtained as

$$|\mathrm{e}^{\eta_1^{[1]}}| = 1, \quad |\mathrm{e}^{\eta_1^{[2]}}| = 1.$$

Utilizing the relation $\boldsymbol{\Psi}_1[1] = \boldsymbol{\Gamma}_1^{[1]}\boldsymbol{\Phi}_1[1]$, the corresponding relations between the three components in the vector function $\boldsymbol{\Psi}_1[1]$ and the ones in the vector function $\boldsymbol{\Phi}_1[1]$ can be derived as

$$\begin{pmatrix} \psi_1[1] \\ \phi_1[1] \\ \chi_1[1] \end{pmatrix} = \begin{pmatrix} \mathrm{e}^{\eta_1^{[1]}}\phi_1^{(1)}[1] \\ \mathrm{e}^{-\eta_1^{[1]}}\phi_1^{(2)}[1] \\ \mathrm{e}^{-\eta_1^{[1]}}\phi_1^{(3)}[1] \end{pmatrix}. \tag{42}$$

Through Eqs. (9) and (14), the module of $q_1[2]$ can be directly generated as

$$\begin{aligned} |q_1[2]| &= \left| \mathrm{e}^{2\eta_1^{[2]}}\left(q_1[1] + \frac{2\mathrm{i}(\lambda_1^* - \lambda_1)\psi_1[1]\phi_1[1]^*}{|\psi_1[1]|^2 + |\phi_1[1]|^2 + |\chi_1[1]|^2}\right)\right| \\ &= \left| q_1[1] + \frac{2\mathrm{i}(\lambda_1^* - \lambda_1)\psi_1[1]\phi_1[1]^*}{|\psi_1[1]|^2 + |\phi_1[1]|^2 + |\chi_1[1]|^2}\right| \\ &= \left| \mathrm{e}^{2\eta_1^{[1]}}\left(q_1[0] + \frac{2\mathrm{i}(\lambda_1^* - \lambda_1)\psi_1[0]\phi_1[0]^*}{|\psi_1[0]|^2 + |\phi_1[0]|^2 + |\chi_1[0]|^2}\right) + \frac{2\mathrm{i}(\lambda_1^* - \lambda_1)\psi_1[1]\phi_1[1]^*}{|\psi_1[1]|^2 + |\phi_1[1]|^2 + |\chi_1[1]|^2}\right| \\ &= \left| q_1[0] + \frac{2\mathrm{i}(\lambda_1^* - \lambda_1)\psi_1[0]\phi_1[0]^*}{|\psi_1[0]|^2 + |\phi_1[0]|^2 + |\chi_1[0]|^2} + \frac{2\mathrm{i}(\lambda_1^* - \lambda_1)\phi_1^{(1)}[1]\phi_1^{(2)*}[1]}{|\phi_1^{(1)}[1]|^2 + |\phi_1^{(2)}[1]|^2 + |\phi_1^{(3)}[1]|^2}\right|, \end{aligned}$$

in a similar way, the validity of Eq. (38) can also be testified.

This completes the proof of Proposition 1. □

By virtue of the above formulae (37) and (38), we can obtain concrete expressions of the modules for the second-order localized wave solutions. Here, we omit presenting the expressions since they are rather cumbersome to write down. According to different values of the free parameters α, d_1, and d_2, we can also obtain three kinds of the second-order nonlinear localized waves of the CCQNLS system (1).[32,33]

(I) $\alpha = 0$, $d_1 \neq 0$, and $d_2 \neq 0$.

Here, the second-order semi-rational solutions degenerate to the rational ones, thus, the second-order rogue wave of the CCQNLS equations can be obtained. When $s_1 = 0$, the second-order rogue wave is fundamental pattern, see Fig. 6; while $s_1 \neq 0$, the the second-order rogue wave is triangular pattern, see Fig. 7.

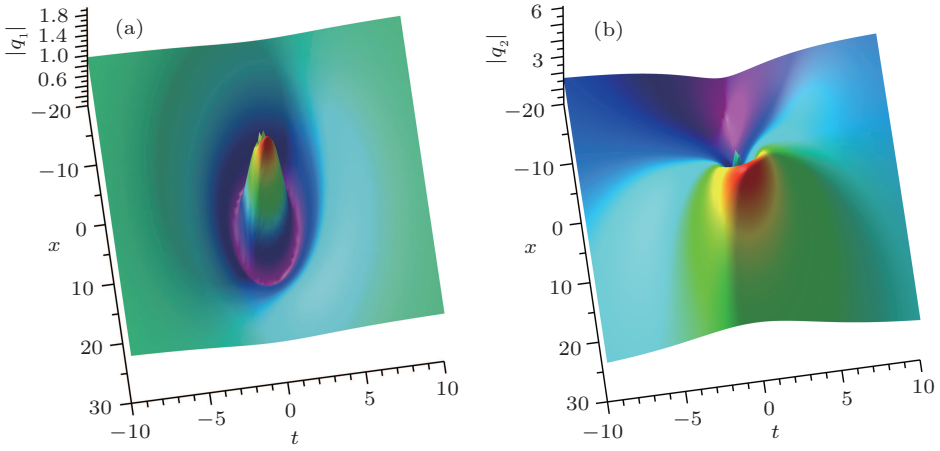


Fig. 6. (color online) Evolution plot of the second-order rogue wave of fundamental pattern in the CCQNLS equations with the parameters chosen by $\alpha = 0$, $\rho_1 = 1/10$, $\rho_2 = 1/20$, $d_1 = 1$, $d_2 = -2$, $m_1 = 0$, $n_1 = 0$: (a) q_1 component,(b) q_2 component.

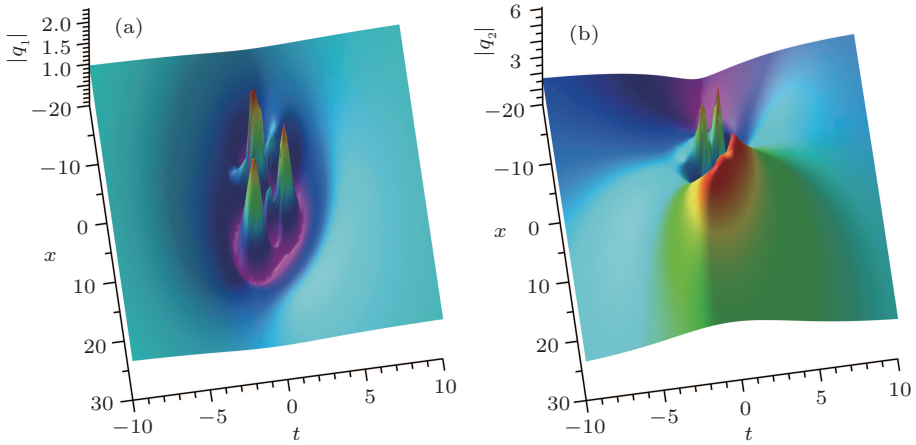


Fig. 7. (color online) Evolution plot of the second-order rogue wave of triangular pattern in the CCQNLS equations with the parameters chosen by $\alpha = 0$, $\rho_1 = 1/10$, $\rho_2 = 1/20$, $d_1 = 1$, $d_2 = -2$, $m_1 = -100$, $n_1 = 100$: (a) q_1 component,(b) q_2 component.

(II) $\alpha \neq 0$, $d_1 = 0$, and $d_2 \neq 0$.

At this point, the first kind of the second-order semi-rational solutions between two dark (bright) solitons and one second-order rogue wave can be given. Figure 8(a) shows two bright solitons together with a fundamental second-order rogue wave, besides, figure 8(b) demonstrates two dark solitons coexisting with a fundamental second-order rogue wave.

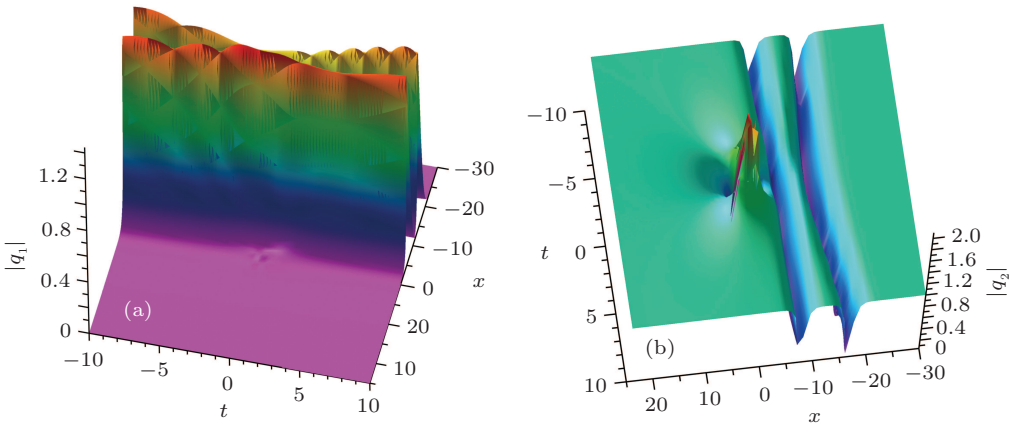


Fig. 8. (color online) Evolution plot of the interactional solution between the second-order rogue wave of fundamental pattern and two-soliton in the CCQNLS equations with the parameters chosen by $\alpha = 1/200$, $\rho_1 = 1/10$, $\rho_2 = 1/20$, $d_1 = 0$, $d_2 = 1$, $m_1 = 0$, $n_1 = 0$. (a) Two bright solitons together with a fundamental second-order rogue wave in q_1 component; (b) Two dark solitons together with a fundamental second-order rogue wave in q_2 component.

In Fig. 8(a), when the two bright solitons interact with the second-order rogue wave, the second-order rogue wave in q_1 component is not observed easily for the same reason as the first-order case. When setting $s_1 \neq 0$, the fundamental second-order rogue wave can split into three first-order rogue waves, in addition, the second-order rogue wave of triangular pattern and two solitons separate in Fig. 9. By increasing the absolute value of α, the two dark (bright) solitons merge with the second-order rogue wave of triangular pattern, see Fig. 10.

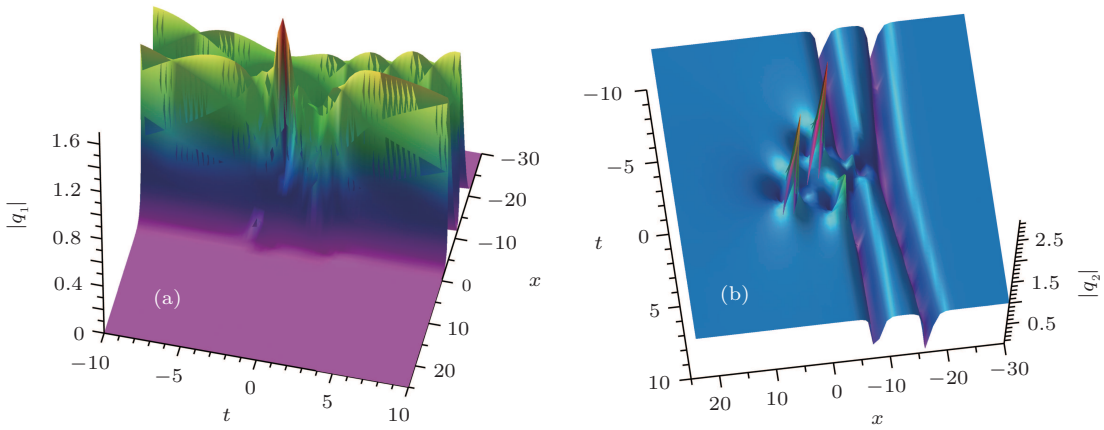


Fig. 9. (color online) Evolution plot of the interactional solution between the second-order rogue wave of triangular pattern and two-soliton in the CCQNLS equations with the parameters chosen by $\alpha = 1/200$, $\rho_1 = 1/10$, $\rho_2 = 1/20$, $d_1 = 0$, $d_2 = 1$, $m_1 = 50$, $n_1 = -50$. (a) Two bright solitons and a second-order rogue wave of triangular pattern separate in q_1 component; (b) Two dark solitons and a second-order rogue wave of triangular pattern separate in q_2 component.

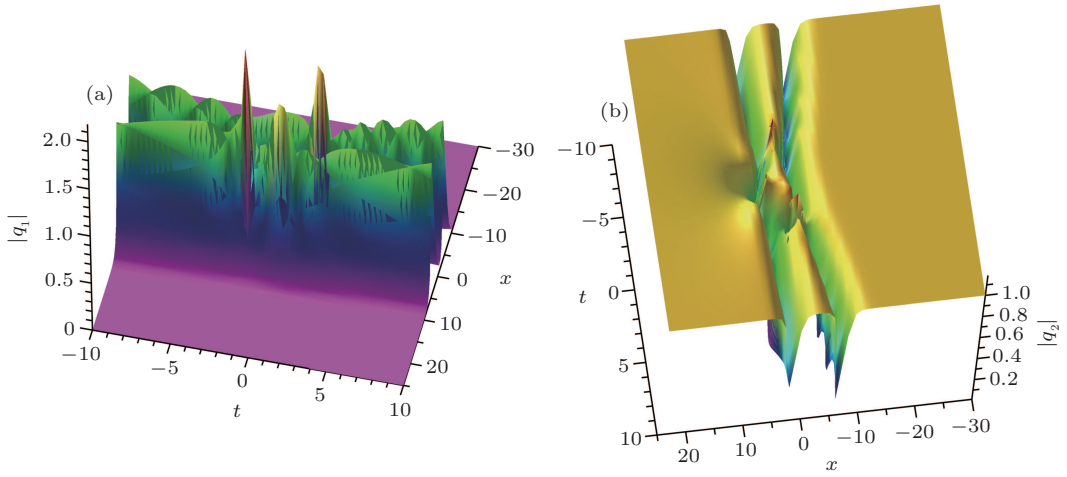


Fig. 10. (color online) Evolution plot of the interactional solution between the second-order rogue wave of triangular pattern and two-soliton in the CCQNLS equations with the parameters chosen by $\alpha = 100$, $\rho_1 = 1/10$, $\rho_2 = 1/20$, $d_1 = 0$, $d_2 = 1$, $m_1 = 50$, $n_1 = -50$. (a) Two bright solitons merge with a second-order rogue wave of triangular pattern in q_1 component; (b) Two dark solitons merge with a second-order rogue wave of triangular pattern in q_2 component.

(III) $\alpha \neq 0$, $d_1 \neq 0$, and $d_2 \neq 0$.

Hence, we arrive at the second kind of the second-order semi-rational solutions between two breathers and a second-order rogue wave in the two components q_1 and q_2, see Figs. 11–13. Meanwhile, setting $s_1 \neq 0$, the fundamental second-order rogue can split into three first-order rogue waves, see Figs. 11 and 12. By decreasing the absolute value of α, it shows that the two parallel breathers and the second-order rogue of triangular pattern separate in Fig. 12. However, increasing the absolute value of α, it demonstrates that the two parallel breathers merge with the second-order rogue wave in Fig. 13.

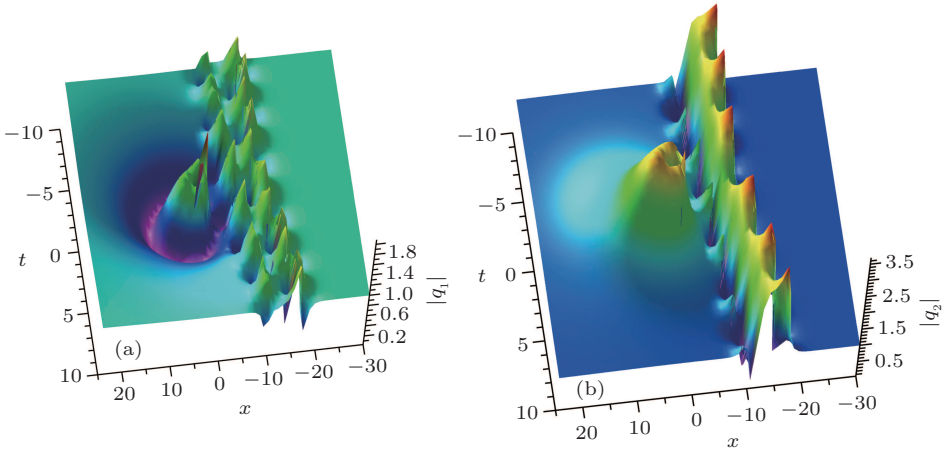


Fig. 11. (color online) Evolution plot of the interactional solution between the second-order rogue wave of fundamental pattern and two-breather in the CCQNLS equations with the parameters chosen by $\alpha = 1/1000$, $\rho_1 = 1/10$, $\rho_2 = 1/20$, $d_1 = 1$, $d_2 = -1$, $m_1 = 0$, $n_1 = 0$. Two parallel breathers and a fundamental second-order rogue wave exist in the two components: (a) q_1 component, (b) q_2 component.

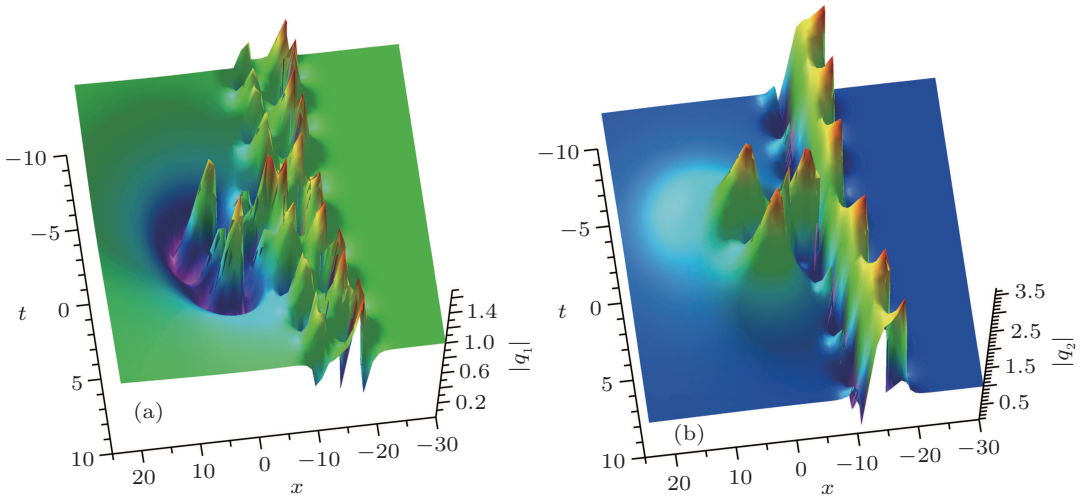


Fig. 12. (color online) Evolution plot of the interactional solution between the second-order rogue wave of triangular pattern and two-breather in the CCQNLS equations with the parameters chosen by $\alpha = 1/1000$, $\rho_1 = 1/10$, $\rho_2 = 1/20$, $d_1 = 1$, $d_2 = -1$, $m_1 = 50$, $n_1 = -50$. Two parallel breathers and a fundamental second-order rogue wave separate in the two components: (a) q_1 component, (b) q_2 component.

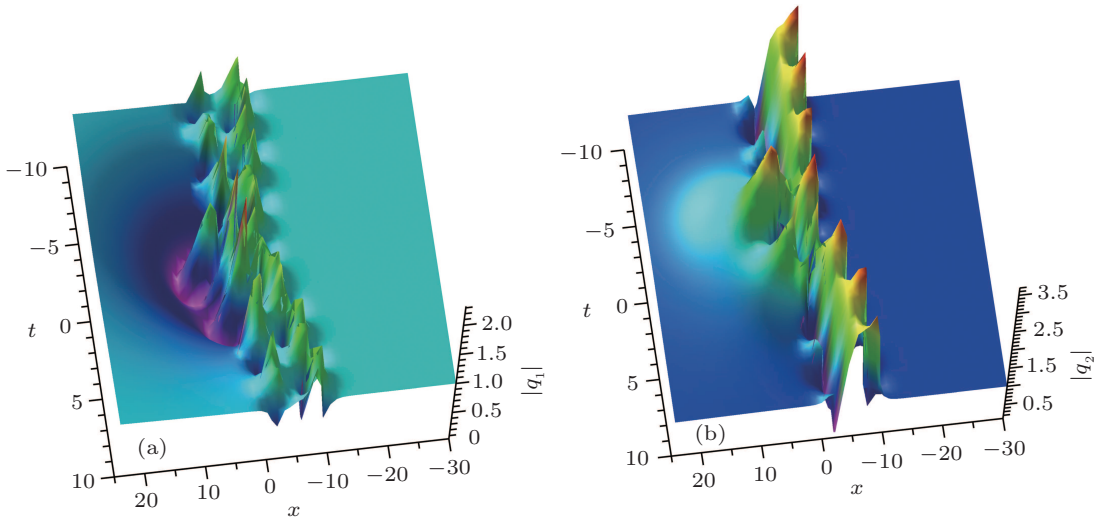


Fig. 13. (color online) Evolution plot of the interactional solution between the second-order rogue wave of triangular pattern and two-breather in the CCQNLS equations with the parameters chosen by $\alpha = 100$, $\rho_1 = 1/10$, $\rho_2 = 1/20$, $d_1 = 1$, $d_2 = -1$, $m_1 = 50$, $n_1 = -50$. Two parallel breathers merge with a fundamental second-order rogue wave in the two components: (a) q_1 component, (b) q_2 component.

Through discussing the different values of the free parameters d_1, d_2, and α in the the first-order localized wave solutions, we can get various kinds of interactional solutions. Instead of considering various arrangements of the two potential functions q_1 and q_2, we consider the same combination as the same type solution. Hence we can get three types of the first-order localized wave solutions using our method: 1) One first-order rogue wave; 2) one dark or bright soliton together with one first-order rogue wave; 3) one breather interacting with one first-order rogue wave. However, the expressions of the second-order localized waves are very tedious and complicated, we do not give these expressions in the general form. The three types of hybrid solutions which are similar with the first-order case are only demonstrated. Whether the second-order localized waves own more types or not, we cannot draw a firm conclusion now.

4. Conclusion

In conclusion, choosing a periodic seed solution of Eq. (1), a peculiar vector solution of the Lax pair (2) is elaborately derived. Based on the special vector solution, we present some interesting and appealing nonlinear localized waves in the CCQNLS equations (1) through the generalized DT. The multi-parametric and semi-rational solutions of Eq. (1) are obtained, where some free parameters play an important role in controlling the dynamic properties of these localized nonlinear waves, such as α, d_1, d_2, and s_i $(i = 1, 2, \ldots, N)$.[32,33] The first- and second-order hybrid solutions of the CCQNLS equations are mainly discussed in three cases: I) when $\alpha = 0$, $d_1 \neq 0$, and $d_2 \neq 0$, the semi-rational solutions degenerate to the rational ones, e.g., the first- and second-order rogue waves; II) when $\alpha \neq 0$, $d_1 = 0$, and $d_2 \neq 0$, the first kind of the higher-order semi-rational solutions are presented, such as hybrid solutions between a first-order rogue

wave and a dark or bright soliton, a second-order rogue wave and two dark or bright solitons; III) when $\alpha \neq 0$, $d_1 \neq 0$, and $d_2 \neq 0$, the second kind of the higher-order semi-rational solutions are shown, such as hybrid solutions between a first-order rogue wave and a breather, a second-order rogue wave and two breathers.

Baronio *et al.*[46] obtained the first-order semi-rational solutions in the coupled NLS, however, the higher-order interactional solutions are not constructed. We construct the higher-order localized wave solutions of the CCQNLS system (1) through the generalized DT. For one thing, iterating the generalized DT process, we can generate more complicated localized wave solutions possessing more abundant striking dynamics. For another thing, there were many other interactional solutions in other nonlinear models.[31–33] The rogue waves together with cnoidal periodic waves in the focusing NLS equation are obtained by DT method.[25] Additionally, a study about rogue waves interacting with solitons and breathers at the same time was published. We will investigate the above two aspects in our future work. Furthermore, we hope that these kinds of nonlinear localized waves of the CCQNLS equations (1) will be verified in physical experiments in the future.

Acknowledgments

We would like to express our sincere thanks to Profs. S Y Lou, Z Y Yan, and E G Fan for their discussions and suggestions. Meanwhile, we express heartfelt thanks to other members of our discussion group for their valuable comments.

References

[1] Zabusky N J and Kruskal M D 1965 *Phys. Rev. Lett.* **15** 240
[2] Hasegawa A and Kodama Y 1995 *Solitons in Optical Communication* (Oxford: Oxford University Press)
[3] Ablowitz M J and Clarkson P A, 1991 *Solitons, Nonlinear Evolution Equations and Inverse Scattering* (Cambridge: Cambridge University Press)
[4] Akhmediev N, Soto-Crespo J M and Ankiewicz A 2009 *Phys. Rev. A* **80** 043818
[5] Ohta Y and Yang J K 2012 *Phys. Rev. E* **86** 036604
[6] Dubard P and Matveev V B 2013 *Nonlinearity* **26** R93
[7] Liu Y K and Li B 2017 *Chin. Phys. Lett.* **34** 10202
[8] Soto-Crespo J M, Devine N and Akhmediev N 2016 *Phys. Rev. Lett.* **116** 103901
[9] Chowdury A, Kedziora D J, Ankiewicz A and Akhmediev N 2015 *Phys. Rev. E* **91** 022919
[10] Forest M G, McLaughlin D W, Muraki D J and Wright O C 2000 *J. Nonlinear Sci.* **10** 291
[11] Ma Y C 1979 *Stud. Appl. Math.* **64** 43
[12] Akhmediev N and Korneev V I 1986 *Theor. Math. Phys.* **69** 1089
[13] Akhmediev N, Ankiewicz A and Taki M 2009 *Phys. Lett. A* **373** 675
[14] Guo B L, Tian L X, Yan Z Y and Ling L M 2015 *Rogue Waves and their Mathematical Theory* (Hangzhou: Zhejiang Science and Technology Press)
[15] Solli D R, Ropers C, Koonath P and Jalali B 2007 *Nature* **450** 54
[16] Akhmediev N, Dudley J M, Solli D R and Turitsyn S K 2013 *J. Opt.* **15** 060201
[17] Shats M, Punzmann H and Xia H 2010 *Phys. Rev. Lett.* **104** 104503
[18] Ganshin A N, Efimov V B, Kolmakov G V, Mezhov-Deglin L P and McClintock P V E 2008 *Phys. Rev. Lett.* **101** 065303
[19] Pitaevskii L and Stringari S 2016 *Bose–Einstein Condensation and Superfluidity* (Oxford: Oxford University Press)
[20] Bailung H and Nakamura Y 1993 *J. Plasma Phys.* **50** 231
[21] Yan Z Y *Phys. Lett. A* **375** 4274
[22] Jia J and Lin J 2012 *Opt. Express* **20** 7469
[23] Ren B and Lin J 2015 *Z. Naturforsch. A* **70** 539
[24] Huang L L and Chen Y 2016 *Chin. Phys. B* **25** 060201
[25] Kedziora D J, Ankiewicz A and Akhmediev N 2014 *Eur. Phys. J. Spec. Top.* **223** 43
[26] Zhang X E and Chen Y 2017 *Commun. Nonlinear Sci. Numer. Simul.* **52** 24
[27] Zhang X E, Chen Y and Tang X Y arXiv: 1610.09507v1
[28] Wang L, Zhu Y J, Wang Z Z, Qi F H and Guo R 2016 *Commun. Nonlinear Sci. Numer. Simul.* **33** 218
[29] Guo B L and Ling L M 2011 *Chin. Phys. Lett.* **28** 110202
[30] Wang X and Chen Y 2014 *Chin. Phys. B* **23** 070203
[31] Xu T and Chen Y 2016 *Chin. Phys. B* **25** 090201
[32] Wang X, Li Y Q and Chen Y 2014 *Wave Motion* **51** 1149
[33] Wang X, Yang B, Chen Y and Yang Y Q 2014 *Chin. Phys. Lett.* **31** 090201
[34] Zhao L C, Yang Z Y and Ling L M 2014 *J. Phys. Soc. Jpn.* **83** 104401
[35] Rao J G, Liu Y B, Qian C and He J S 2017 *Z. Naturforsch. A* **72**
[36] Wang P and Tian B 2012 *Opt. Commun.* **285** 3567
[37] Qi F H, Tian B, Lü X, Guo R and Xue Y S 2012 *Commun. Nonlinear Sci. Numer. Simul.* **17** 2372
[38] Zhang Y, Nie X J and Zha Q L 2014 *Phys. Lett. A* **378** 191
[39] Wang Y F, Tian B, Sun W R and Liu X R 2016 *Optik* **127** 5750
[40] Kundu A 1984 *J. Math. Phys.* **25** 3433
[41] Huang G Q and Lin J 2017 *Acta Phys. Sin.* **66** 054208 (in Chinese)
[42] Geng X G 1999 *Physica A* **180** 241
[43] Geng X G and Tam H W 1999 *J. Phys. Soc. Jpn.* **68** 1508
[44] Zha Q L 2013 *Phys. Lett. A* **377** 855
[45] Wang X, Yang B, Chen Y and Yang Y Q 2014 *Phys. Scr.* **89** 095210
[46] Baronio F 2012 *Phys. Rev. Lett.* **109** 044102
[47] Matveev V B 1991 *Darboux Transformations and Solitons* (New York: Springer-Verlag)